

Spectroscopic Inline Thermometry

T. Tomberg, T. Hieta, T. Fordell, M. Merimaa

VTT Technical Research Centre of Finland Ltd, Centre for Metrology MIKES, P.O. Box 1000, FI-02044 VTT, Finland

Abstract. In optical distance measurements it is essential to know the refractive index of air with high accuracy. Commonly, the refractive index of air is calculated from the properties of the ambient air using either Ciddor or Edlén equations, where the dominant uncertainty component is in most cases air temperature. The method described in this contribution utilizes direct absorption laser spectroscopy of oxygen to measure the average temperature of air over long distances. The method allows measurement of temperature over the same beam path that is used for the optical distance measurement, which yields spatially well matching data. Indoor and outdoor measurements demonstrate the effectiveness of the developed method in compensating local temperature variations along the measurement path.

Our work in the EMRP JRP SIB60 Surveying project aims to extend the measurement distance of oxygen thermometry up to 1 km using a simplified single-laser setup for extra robustness and simplicity. The new setup designed for field applications include larger diameter optics and a separate transmitting and receiving end. The developed instrument was tested at Nummela geodetic baseline in a measurement campaign in Sep/Oct 2015. The goal was to determine the effective temperature of the air with a precision at the 100 mK level using modest averaging (<5 min).

Keywords. EMRP JRP SIB60 Surveying, refractive index of air, air temperature, laser spectroscopy

1 Introduction

Tunable diode laser absorption spectroscopy (TDLAS) is a well-known sensitive technique used for measuring gas concentration down to trace levels. The depth, width and position of an absorption line depend on, e.g., temperature T , pressure p and gas mixture and velocity, which, in turn, implies that in addition to gas density N , temperature, pressure and velocity can also be determined spectroscopically. Temperature is an important parameter in combustion, and thus, most

of the effort in developing spectroscopic methods for temperature determination has been directed towards techniques that work at elevated temperatures: from hundreds to several thousands of degrees (Chang et al. (1987), Philippe and Hanson (1993), Arroyo and Hanson (1993), Benedetti et al. (1998), Silver and Kane (1999), Ebert et al. (2000), Sanders et al. (2001), Aizawa (2001), Zhou et al. (2003), Liu et al. (2004), Zhou et al. (2005), Shao et al. (2008)).

The refractive index of air is also sensitive to temperature, and thus, accurate temperature readings are needed in precision length metrology as well. A 1-K change in temperature results in a 10^{-6} change in the refractive index, and the best equations for the refractive index are believed to be accurate at the 10^{-8} level if sufficiently accurate environmental parameters are available (Birch and Downs (1994), Ciddor (1996), Bönsch and Potulski (1998)); therefore, for best accuracy, the effective temperature seen by distance measuring laser beams should be known at the 10 mK level. In laboratory conditions this is not a big problem, but for long distance measurements in the field, obtaining accurate temperature readings over the entire distance to be measured may become problematic, especially if large gradients might be present due to, e.g., sunlight (Pollinger et al. (2012)).

The sensitivity of electronic distance meters (EDMs) to temperature can be reduced significantly by measuring at two (see e.g. Meiners-Hagen et al. (2015), Kang et al. (2015)) or three wavelengths (Golubev and Chekhovskiy (1993)) with the added complexity being a drawback. Also, to reach 10^{-7} in distance uncertainty, which is the target for the present project, the allowed uncertainty in relative humidity is reduced from 12 % for a one-color measurement to only 4 % for two-colors (Minoshima et al. (2010)). An alternative is to try to measure the effective temperature seen by the distance measuring laser beam, and to use that to estimate the effective refractive index.

2 The Refractive Index and Temperature

Suppose distance is measured with a continuous-wave laser interferometer. Then, the phase $\Delta\Phi$ acquired over a distance L is given by

$$\begin{aligned}\Delta\Phi &= \frac{2\pi}{\lambda} \int_0^L n(T(x), p_{tot}(x), \dots) dx \\ &= \frac{2\pi}{\lambda} \langle n(T(x), p_{tot}(x), \dots) \rangle L,\end{aligned}\quad (1)$$

where λ is the vacuum wavelength, n is the refractive index, T is the temperature, p_{tot} is the total pressure, L is the length and $\langle \rangle$ denotes an average along the path. If all parameters except the temperature are assumed constant along the measurement path, and the temperature is expressed as a deviation from its true mean along the path,

$$T(x) = \langle T \rangle + \Delta T(x), \quad (2)$$

then, based on Eq. (1) we get

$$\begin{aligned}\Delta\Phi &\approx \frac{2\pi L}{\lambda} (n(\langle T \rangle) + \frac{1}{2} \partial_T^2 n \langle \Delta T(x)^2 \rangle) \\ &\approx \frac{2\pi L}{\lambda} (n(\langle T \rangle) + 3 \cdot 10^{-9} / K^2 \langle \Delta T^2 \rangle).\end{aligned}\quad (3)$$

The small correction arises because the refractive index is nonlinear in T . The correction is, however, smaller than the accuracy of n (10^{-8}) for reasonable temperature gradients. If, say, there is a 2-K linear temperature increase along the measurement path, then

$$\langle \Delta T^2 \rangle = \frac{1}{3} K^2, \quad (4)$$

and the first order correction is at the 10^{-9} level. Unless there are considerable gradients along the measurement path, the average temperature can be used in the calculation of the refractive index.

2.1 Two-Line Thermometry

The Beer-Lambert law relates the transmitted intensity $I(v, T(x), p_{tot}, p_{abs}, \dots, L)$ to the incident intensity I_0 via the absorbance $\alpha(v, T(x), p_{tot}, p_{abs}, \dots)$:

$$I(v, T(x), p_{tot}, p_{abs}, \dots) = I_0 e^{-\int_0^L \alpha(v, T(x), p_{tot}, p_{abs}, \dots) dx}, \quad (5)$$

where ν is the frequency, p_{tot} is the total pressure and p_{abs} the partial pressure of the absorbers. The absorbance can be expressed as

$$\begin{aligned}\alpha(\nu, T(x), p_{tot}, p_{abs}, \dots) &= \\ S_i(T) g(\nu, T(x), p_{tot}, p_i, \dots) N(T(x), p_{abs}),\end{aligned}\quad (6)$$

where $S_i(T)$ is the line intensity, $g(\nu, T(x), p_{tot}, p_{abs}, \dots)$ is the area-normalized line shape function and $N(T(x), p_{abs})$ is the number density of absorbers, which can be computed from the partial pressure via the ideal gas law:

$$N(T(x)) = \frac{p_{abs}}{k_B T(x)}. \quad (7)$$

At optical frequencies, the line strength $S_i(T)$ can be expressed as (Rothman et al. (1998)):

$$S_i(T) \approx S_i(T_{ref}) \frac{Q(T_{ref})}{Q(T)} e^{-\frac{E_i}{k_B} \left(\frac{1}{T} - \frac{1}{T_{ref}} \right)}, \quad (8)$$

where T_{ref} is a reference temperature, $Q(T)$ is the total internal partition function, E_i is the lower state energy and k_B is the Boltzmann constant. Approximate third order polynomials for $Q(T)$ for molecules in the terrestrial atmosphere have been calculated by Gamache et al. (2000).

In a direct absorption experiment the transmitted intensity I is normalized with the output, and after a logarithm this gives access the absorbance:

$$\begin{aligned}-\ln(I/I_0) &= L \frac{1}{L} \int_0^L \alpha(\nu, T(x), p_{tot}, p_i, \dots) dx \\ &= L \langle \alpha(\nu, T(x), p_{tot}, p_i, \dots) \rangle,\end{aligned}\quad (9)$$

If, for the moment, T is assumed to be constant, then integration over the absorption line (or fitting $g(\nu, T, p_{tot}, p_{abs}, \dots)$ to the signal) gives

$$\begin{aligned}\langle \alpha(\nu, T, p_{tot}, p_i, \dots) \rangle &= \left\langle \frac{S_i(T) N(T, p_i)}{L} \int g(\nu, T, p_{tot}, p_i, \dots) d\nu \right\rangle \\ &= S_i(T) N(T, p_i) / L\end{aligned}\quad (10)$$

since $g(\dots)$ is area-normalized to unity. In two-line thermometry, the ratio R of two different absorption

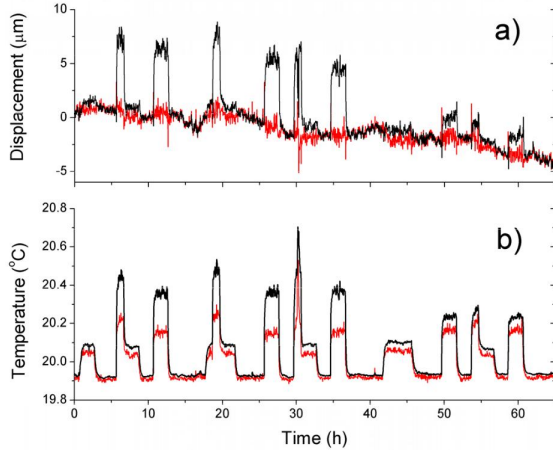


Fig. 1. Refractive index compensation over a 30-m measurement path with artificially induced temperature gradients. Part (a) shows the results using spectroscopic temperature data (red) and temperature data from eight Pt-100 sensors (black). Part (b) shows the average temperature along the path. This figure is reproduced from Hieta et al. (2011) with permission from the publisher.

lines is measured in order to get rid of the concentration dependency:

$$R = \frac{S_2(T)N(T, p)}{S_1(T)N(T, p)} = \frac{S_2(T)}{S_1(T)} \approx \frac{S_2(T_{ref})}{S_1(T_{ref})} e^{\left[\frac{E_2 - E_1}{k} \left(\frac{1}{T} - \frac{1}{T_{ref}} \right) \right]} \quad (11)$$

With known values for $S_{1,2}$, $E_{1,2}$ and T_{ref} the temperature can be determined; however, the correctness of tabulated values should be carefully assessed. Also, finding suitable, background-free absorption lines can be very challenging especially at elevated temperatures (Zhou et al. (2003), Zhou et al. (2005)). To get around this obstacle, the use of two groups of lines has been explored by Shao et al. (2009) with encouraging results.

As mentioned in the introduction, a lot of work has been put into the development of spectroscopic thermometers for the elevated temperatures that are of interest in the study of combustion. Hieta and Merimaa (2010) developed a thermometer based on oxygen spectroscopy at 760 nm for the compensation of the refractive index in length measurements, and in a follow-up paper by Hieta et al. (2011), it was demonstrated that the spectroscopic thermometer was able to compensate

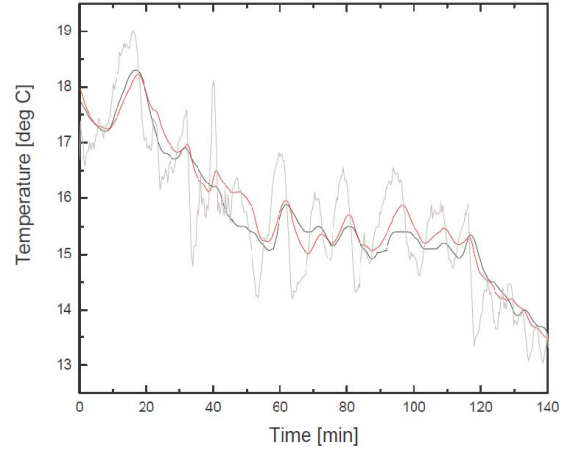


Fig. 2. Spectroscopic single-line temperature measurement performed at the Innsbruck geodetic baseline over a path length of 2x120m. The spectroscopic temperature using 20 s sample time is shown in grey. The low-pass filtered spectroscopic temperature and reference sensor data are marked with red and black lines, respectively.

for the changing refractive index much better than an ensemble of Pt-100 sensors when temperature gradients were artificially introduced into the measurement path. Figure 1 shows the results over a 30-m measurement path. Even eight Pt-100 sensors (black) were not enough to accurately account for the changing temperature. The spectroscopic method in red, however, is able to accurately correct for the temperature gradients.

The equations yielding the temperature from the absorbance are nonlinear and it is not obvious that the resulting temperature is the average temperature. It is, however, an easy matter to show as in section 2 that the first correction to the absorbance is $\approx 10^{-5} \langle \Delta T^2(x) \rangle$, which is negligible for reasonable temperature gradients (e.g. 1 mK for a gradient of a few Kelvins along the path).

2.2 Single-Line Thermometry

If accurate values for the line strengths that are needed in the ratio measurement are not available, then a calibration is needed over a relevant range of temperatures in order to determine the scaling factor $S_2(T_{ref})/S_1(T_{ref})$. Then, the remaining advantage of using two-lines instead of a single line is that the ratio measurement is insensitive to changes in concentration. If, however, the concentration is

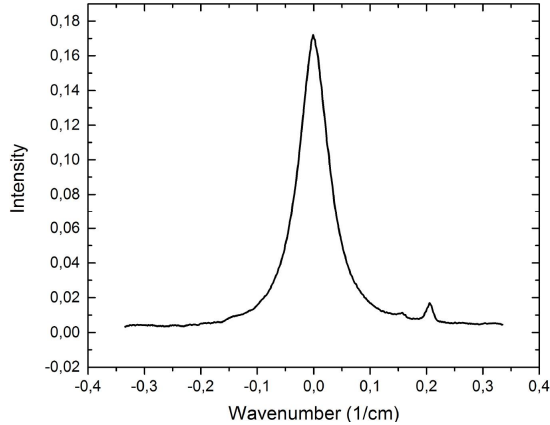


Fig. 3. Oxygen absorption at 13000.0 cm^{-1} (769.23 nm) over a distance of 432 m . The small features at 0.15 and 0.2 cm^{-1} are due to the beam being blocked by, e.g., an insect or a falling leaf.

known, then a single-line measurement might be sufficient.

Atmospheric $\delta\text{O}_2/\text{N}_2$ ratio measurements show only a small ≈ 20 per meg average annual decrease together with an annual oscillation of up to ± 50 per meg (Keeling and Shertz (1992), Manning and Keeling (2006)), which suggests that temperature can be determined outdoors using single-line oxygen spectroscopy. The relative sensitivity of the spectroscopy signal is of the order of $1 \text{ \%}/\text{K}$ so that a 100 mK target accuracy still leaves room for larger local O_2 variations that might take place.

Figure 2 shows the results from a thermometer based on single-line oxygen thermometry that was tested at the Innsbruck geodetic baseline over a $2 \times 120 \text{ m}$ distance. The spectroscopic temperature using 20 s sample time is shown in grey. The low-pass filtered spectroscopic temperature and reference sensor data are given in red and black, respectively. Unfortunately, laser temperature controller instabilities prevented the use of the same transition as used in the calibration of the device; therefore, the line strength $S(T_{ref})$ and E were used as free parameters (Eq. 8).

Since the spectrometer is based on measurement of the transmitted light, any beam clipping by the optics will seriously reduce the signal quality. Indeed, at Innsbruck the path length was limited by the $2''$ optics used to launch and detect the laser beams.

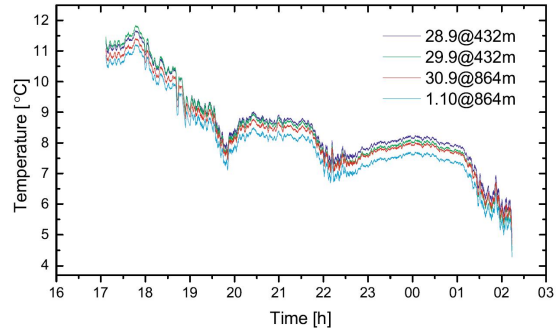


Fig. 4. Preliminary temperature data for September 28 over a distance of 432 m . The different lines indicate calibration of $S(T_{ref})$ and E in Eq. 8 using data from different days.

3 Towards a 1 km Path Length

A small part of the ongoing European Metrology Research Project SIB60 Surveying aims at extending the measurement distance of oxygen thermometry up to 1 km . The new setup designed for field applications included larger diameter optics and a separate transmitting and receiving end.

3.1 The Setup

Light from a distributed feedback diode laser is amplitude modulated by an electro-optic modulator, and split into three branches: in the first branch, transmission modulation resulting from a 30-cm fiber with FC/PC connectors (a fiber etalon that is) is used to monitor the frequency sweep of the laser; the second branch is used as the reference (I_0 in Eq. (5)), and the third ‘spectroscopy’ branch is collimated with an aspheric lens with diffraction limited performance. A focal length of 200 mm results in a maximum waist distance of 780 m and a $1/e^2$ spot diameter of 25 mm at 1 km . Air turbulence will surely increase this value; therefore, a collecting lens with a large 200 mm aperture and a 40 cm focal length was used. Fortunately, a low quality, inexpensive lens is sufficient in the receiver, where a photodiode detects the light and sends it via a differential amplifier and a shielded and twisted pair cable (Ethernet Cat 6 cable) back to the transmitting end where two SR830 lock-in amplifiers detect the signal and the reference.

An example of an absorption signal after a distance of 432 m is shown in Fig. 3. At wavenumbers

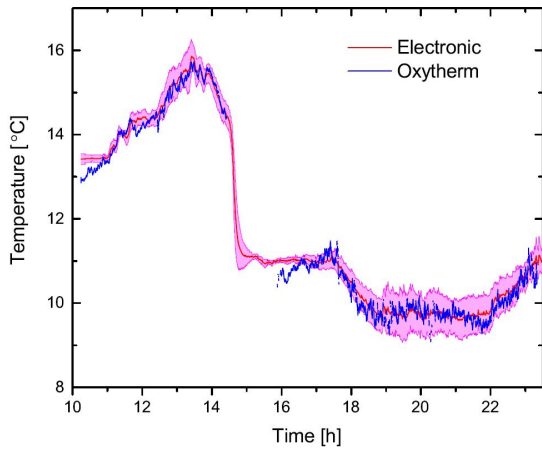


Fig. 5. Spectroscopically determined temperature over a distance of 864 m. Here, $S(T_{ref})$ and E have been treated as free parameters in the fit to the average temperature measured by four Pt-100 sensors (pink).

0.15 cm^{-1} and 0.2 cm^{-1} typical features are seen: the beam has been blocked by, e.g., falling leaves or insects during the frequency scan.

3.2 Temperature

Figure 4 shows preliminary temperature results. Data obtained on Sep 28 (432 m) has been calibrated using data from four different days. When the calibration is performed using 432 m data taken on Sep 29, an offset of approx. 100 mK is obtained; however, when the calibration is done using data from the 864 m measurements, this offset is increased up to 0.5 K. A preliminary analysis suggests that this discrepancy between the distances is due to beam blocking events such as those shown in Fig. 3. When the beam is blocked, the blockage is always seen as a reduction in transmission. When this happens on the wings of the absorption line, the algorithm (fitting of $g(\dots)$ in Eq. 10) sees it as an increase in the baseline and thus as a reduction of oxygen absorption. When the beam is blocked close to the peak of the absorption line, the effect is reversed (increased absorption) but the effect is also amplified. Beam interruptions are thus interpreted on average as an increase in absorption, and the longer the path length, the more beam interruptions there are, which, in turn, is seen as a temperature offset.

The signal analysis algorithm needs to be improved so that this effect is removed. Also, any offsets in the reference or spectroscopy electronics will result in offsets and need to be taken into account, or, preferably, should be automatically nulled by the apparatus during the measurements.

Figure 5 shows the performance of the spectroscopic thermometer over a distance of 864 m (blue). At around 14:30 the spectroscopic measurement was interrupted by rainfall. Here $S(T_{ref})$ and E were treated as free parameters. The figure also shows the average temperature and standard deviation of four Pt-100 sensors (pink).

4 Conclusions

In conclusion, a brief introduction to thermometry based on direct absorption spectroscopy has been given with emphasis on refractive index compensation for long distance length metrology. In laboratory conditions, this approach has been shown to effectively account for artificially induced temperature gradients along the measurement path, and based on a preliminary analysis of data obtained outdoors at the Nummela geodetic baseline, the spectroscopic method seems suitable for long distance thermometry up to several kilometers.

References

- Aizawa, T. (2001). Diode-Laser Wavelength-Modulation Absorption Spectroscopy For Quantitative In Situ Measurements of Temperature and OH Radical Concentration in Combustion Gases. *Applied Optics* 40, pp. 4894-4903.
- Arroyo, M.P., and R.K. Hanson (1993). Absorption Measurements of Water-Vapour Concentration, Temperature, and Line-Shape Parameters Using a Tunable InGaAsP Diode Laser. *Applied Optics* 32, pp. 6104-6116.
- Benedetti, R., K. Giuletti, and M. Rosa-Clot (1998). Line Shape Analysis of O₂ in Air as a Way to Measure Temperature Using a DFB-Diode-Laser at 761 nm, *Optics Communications* 154, pp. 47-53.
- Birch, K.P., and M.J. Downs (1994). Correction to the updated Edlén Equation for the Refractive Index of Air. *Metrologia* 30, pp. 315-316.
- Bönsch, G., and E. Potulski (1998), Measurement of the Refractive Index of Air and Comparison with Modified Edlén's Formula. *Metrologia* 35, pp. 133-139.
- Cassidy, D.T., and J. Reid (1982). Atmospheric Pressure Monitoring of Trace Gases Using Tunable Diode Lasers. *Applied Optics* 21, pp. 1185-1190.

- Chang, A.Y., E.C. Rea, and R.K. Hanson (1987). Temperature Measurements in Shock Tubes Using a Laser-Based Absorption Technique. *Applied Optics* 26, pp. 885-891.
- Ciddor, P.E. (1996). Refractive Index of Air: New Equations for the Visible and Near Infrared. *Applied Optics* 35, pp. 1566-1573.
- Ebert, V., T. Fernholz, C. Giesemann, H. Pitz, H. Teichert, J. Wolfrum, and H. Jaritz (2000). Simultaneous Diode-Laser-Based in Situ Detection of Multiple Species and Temperature in a Gas-Fired Power Plant. In: Proc. of the Combustion Institute 28, pp. 423-430.
- Gamache, R.R., S. Kennedy, R. Hawkins, L.S. Rothman (2000). Total Internal Partition Sums for Molecules in the Terrestrial Atmosphere. *Journal of Molecular Structure* 517-518, pp. 407-425.
- Golubev, A.N., and A.M. Chekhovskiy (1994). Three-Color Optical Finding. *Applied Optics* 33, pp. 7511-7517.
- Hieta, T., and M. Merimaa (2010). Spectroscopic Measurement of Air Temperature. *International Journal of Thermophysics* 31, pp. 1710-1718.
- Hieta, T., M. Merimaa, M. Vainio, J. Seppä, A. Lassila (2011). High-Precision Diode-Laser-Based temperature Measurement for Air Refractive Index Compensation. *Applied Optics* 50, pp. 5990-5998.
- Hosseinzadeh, S., and A. Khorsandi (2014). Apodized 2f/1f Wavelength Modulation Spectroscopy Method for Calibration-Free Trace Detection of Carbon Monoxide in the Near-Infrared Region: Theory and Experiment. *Applied Physics B* 116, pp. 521-531.
- Kang, H.J., B.J. Chun, Y.-S. Jang, Y.-J. Kim, and S.-W. Kim (2015). Real-Time Compensation of the Refractive Index of Air in Distance Measurement. *Optics Express* 23, pp. 26377-26385.
- Keeling and Shertz (1992). Seasonal and Interannual Variations in Atmospheric Oxygen and Implications for the Global Carbon Cycle. *Nature* 358, pp. 723-727.
- Liu, J.T., J.B. Jeffries, and R.K. Hanson (2004). Large-Modulation-Depth 2f Spectroscopy with Diode Lasers for Rapid Temperature and Species Measurement in Gases with Blended and Broadened Spectra. *Applied Optics* 43, pp. 6500-6509.
- Manning and Keeling (2006). Global Oceanic and Land Biotic Carbon Sinks From the Scripps Atmospheric Oxygen Flask Sampling Network. *Tellus* 58B, pp. 95-116.
- Meiners-Hagen, K., Bosnjakovic, A., Köchert, P., Pollinger, F. (2015). Air Index Compensated Interferometer as a Prospective Novel Primary Standard for Baseline Calibrations. *Measurement Science and Technology*, 26, 084002.
- Monoshima, K., K. Arai, and H. Inaba (2010). High-Accuracy Self-Correction of Refractive Index of Air Using Two-Color Interferometry of Optical Frequency Combs. *Optics Express* 19, pp. 26095-26105.
- Philippe, L.C., and R.K. Hanson (1993). Laser Diode Wavelength-Modulation Spectroscopy for Simultaneous Measurement of Temperature, Pressure, and Velocity in Shock-Heated Oxygen Flows. *Applied Optics* 32, pp. 6090-6103.
- Pollinger, F., Meyer, T., Beyer, J., Doloca, N.R., Schellin, W., Niemeier, W., Jokela, J., Häkli, P., Abou-Zeid, A., Meiners-Hagen, K. (2012). The Upgraded PTB 600 m Baseline: a High-Accuracy Reference for the Calibration and the Development of Long Distance Measurement Devices. *Measurement Science and Technology*, 23, 094018.
- Rothman, L.S., C. P. Rinsland, A. Goldman, S.T. Massie, D.P. Edwards, J.-M. Flaud, A. Perrin, C. Camy-Peyret, V. Dana, J.-Y. Mandin, J. Schroeder, A. McCann, R. R. Gamache, R.B. Wattson, K. Yoshino, K.V. Chance, K.W. Jucks, L.R. Brown, V. Nemtchinov, P. Varanasi (1998). The HITRAN Molecular Spectroscopic Database and HAWKS (HITRAN Atmospheric Workstation): 1996 Edition. *Journal of Quantitative Spectroscopy and Radiative Transfer* 60, pp. 665-710.
- Sanders, S.T., J. Wang, J.B. Jeffries, and R.K. Hanson (2001). Diode-Laser Absorption Sensor for Line-of-Sight Gas Temperature Distributions. *Applied Optics* 40, pp. 4404-4415.
- Shao, J., L. Lathdavong, P. Kluczynsky, S. Lundqvist, and O. Axner (2009). Methodology for Temperature Measurement in Water Vapor Using Wavelength-Modulation Tunable Diode Laser Absorption Spectrometry in the Telecom C-band. *Applied Physics B* 97, pp. 727-748.
- Silver, J.A., and D.J. Kane (1999). Diode Laser Measurements of Concentration and Temperature in Microgravity Combustion. *Measurement Science and Technology* 10, pp. 845-852.
- Zhou, X., J.B. Jeffries, and R.K. Hanson (2005). Development of a Fast Temperature Sensor for Combustion Gases Using a Single Tunable Diode Laser. *Applied Physics B* 81, pp. 711-722.
- Zhou, X., X. Liu, J.B. Jeffries, and R.K. Hanson (2003). Development of a Sensor for Temperature and Water Vapour Concentration in Combustion Gases Using a Single Tunable Diode Laser. *Measurement Science and Technology* 14, pp. 1459-1468.